AIAA 2008-5893

A Geostatistical Perspective for the Surrogate-Based Integration of Variable Fidelity Models

Efrain Nava[1], Salvador Pintos[2], and Nestor V. Queipo[3]

Applied Computing Institute, University of Zulia, Venezuela

When constructing surrogate models, time/cost constraints make the designer frequently face the dilemma of whether to use a small sample of data obtained from, for example, high fidelity/computationally expensive computer simulations, or, a large one but with low fidelity values. More generally, variable fidelity samples can be the result of: i) different physical/mathematical representations (e.g., inviscid/Euler versus viscous/Navier-Stokes calculations), ii) alternative resolution models (e.g., fine/coarse grids), or, iii) experiments. Ideally, surrogate models should allow: a) the integration of variable-fidelity samples, and, b) provide estimation and appraisal (error) information consistent with the amount and fidelity level of the available data. While there have been significant progress in this area through deterministic modeling and optimization approaches (e.g., correction surfaces, and space mapping), a stochastic perspective such as those provided by the branch of spatial statistics known as geostatistics offers distinctive advantages when satisfying the above referenced requirements (a & b). This paper discusses the effectiveness and requirements of geostatistical methods such as classic and collocated Cokriging for the integration of variable fidelity models. The discussion is illustrated using well-known analytical functions and, alternative resolution models, in the surrogate-based modeling of a field scale alkali-surfactant-polymer (ASP) enhanced oil recovery (EOR) process.

Nomenclature

KRI	=	Ordinary Kriging
CLC	=	Classic Cokriging
CC	=	Collocated Cokriging
Cov	=	Covariance function
Var	=	Variance function
R	=	Correlation function
g	=	Variogram function
F1	=	Analytical case study
ASP	=	Alkali-Surfactant-Polymer
EOR	=	Enhanced oil recovery
NP	=	Cumulative oil production
RMSE	=	Root mean square error
a, b	=	weights of the high and low fidelity samples
Z, V	=	High and low fidelity model samples
s_Z^2, s_V^2	=	High and low fidelity model sample variances
$\hat{z}_0$	=	High fidelity model estimate
v_0	=	Low fidelity model output at prediction sites

[1] Research Engineer, Applied Computing Institute, University of Zulia, Maracaibo, ZU, 4011, Venezuela
[2] Professor, Applied Computing Institute, University of Zulia, Maracaibo, ZU, 4011, Venezuela
[3] Professor and Director, Applied Computing Institute, University of Zulia, Maracaibo, ZU, 4011, Venezuela

I. Introduction

Surrogate modeling is increasingly popular and has been successfully used in the analysis and optimization of computationally expensive models in, for example, the aerospace [1-4], automotive [5,6], and oil industries [7,8]. Recent review papers on the subject are those of Li and Padula[3], G. Gary Wang[9], and, Queipo et al.[4]. When constructing surrogate models, time/cost constraints make the designer frequently face the dilemma of whether to use a small sample of data obtained from, for example, high fidelity/computationally expensive computer simulations, or, a large one but with low fidelity values. More generally, variable fidelity samples can be the result of: i) different physical/mathematical representations (e.g., inviscid/Euler versus viscous/Navier-Stokes calculations), ii) alternative resolution models (e.g., fine/coarse grids), or, iii) experiments. Ideally, surrogate models should allow: a) the integration of variable-fidelity samples, and, b) provide estimation and appraisal (error) information consistent with the amount and fidelity level of the available data.

There have been significant progress in this area through deterministic modeling and optimization approaches such as correction surfaces[10-13] and space mapping[14,15]; however, these alternatives do not provide appraisal (error) information. From a stochastic perspective, geostatistical methods offer distinctive advantages for addressing issues a) and b), most notably: they are founded on solid statistical principles, can be extended to higher dimensions, provide both estimation and error information, the locations of the low and high fidelity data do not have to coincide (i.e., can be non-collocated), represent linear estimators which make them easy to implement through matrix operations, and the estimators can be efficiently updated as new data become available. The required covariance models (structure and parameters) of the variable fidelity data can be identified either through the so called DACE[16] or, variogram approaches.

While there is a variety of geostatistical methods[17-19] potentially useful for addressing the problem of interest such as (increasingly complex): kriging with external drift (KED), collocated cokriging with Markov models (CCM), collocated cokriging (CC), classic cokriging (CLC), in this work, the more general CC and CLC methods are selected for investigation. Related works include those of Kennedy and O´Hagan[20] which was restricted to a CCM method, and those reported in Refs. 21-23 where cokriging approaches use gradient (secondary) information in surrogate-based estimations.

This paper discusses the effectiveness and requirements of geostatistical methods such as collocated (two versions) and classic cokriging for the integration of two level (low and high) fidelity models. The discussion is illustrated using a well-known analytical function and, two distinct resolution models, in the surrogate-based modeling of a field scale alkali-surfactant-polymer (ASP) enhanced oil recovery (EOR) process. ASP flooding is the most promising EOR solution for one of the greatest challenges facing the oil industry worldwide: after conventional water flooding the residual oil (drops trapped by capillary forces) in reservoirs around the world is likely to be around 70 % of the original oil in place.

II. Problem definition

Given $Z = \{z_1, z_2, ..., z_n\}$, and, $V = \{v_1, v_2, ..., v_m\}$, representing high and low fidelity model input/output pairs, respectively, with $m >> n$, build a surrogate of the high fidelity model that provides estimation and appraisal (error) information consistent with the amount and fidelity level of the available data. It is assumed that: i) the high and low fidelity models are correlated, and, ii) each model output is a scalar.

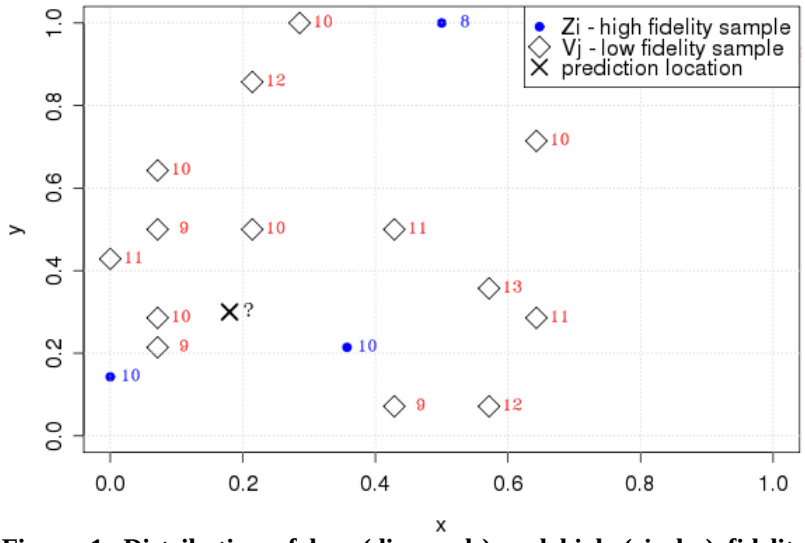

Figure 1. Distribution of low (diamonds) and high (circles) fidelity model sample for a 2D illustration of the problem of interest

Figure 1 shows a particular case of the problem of interest where high (circle) and low (diamond) fidelity model samples are available, and an estimation of the high fidelity model output and corresponding appraisal (error) information is sought at a specific location (marked with an "X").

III. Geostatistical methods

Kriging and related methods represent, so called, BLUE-best (minimum error variance) linear unbiased estimators[17-19]. From the variety of geostatistical methods potentially useful for addressing the problem of interest such as (increasingly complex): kriging with external drift (KED), collocated cokriging with Markov models (CCM), collocated cokriging (CC), classic cokriging (CLC), in this work, the more general CC and CLC methods are selected for investigation.

A. Kriging and Cokriging

Table 1 summarizes the optimization problem associated with Ordinary Kriging, and Classic and Collocated Cokriging, and the corresponding closed-form solutions. In general, the Cokriging methods consider only a small sample associated with a high fidelity model, and, an abundant sample associated with a low fidelity one.

Note that: i) the geostatistical method estimates are linear combinations of the available data, and the main goal of the optimization problem is to find the weights to ensure the best unbiased estimation, and ii) the optimization problems and closed-form solutions assume that a covariance function (*Cov*) has been identified (this issue is addressed later in this section).

Kriging is a spatial prediction method from Geostatistics developed by Matheron[24] and named after the pioneering work of D.G. Krige (a South African mining engineer); Sacks et al.[16,25], and Jones et al.[26] made it well-known in the context of the modeling and optimization of deterministic functions, respectively. In this context, the prediction is modeled as the sum of two effects, a mean (constant or a linear trend), and fluctuations around the mean, and it represents a so called BLUE-best (minimizes prediction error variance) linear unbiased (expected value of the error equal to zero) estimator. Depending on the mean assumption, there are several Kriging formulations, namely, Simple, Ordinary, Universal and Kriging with External Drift; the assumptions: a known constant, a constant (unknown), a linear polynomial on the input variables, and a linear polynomial on an external (secondary) variable, respectively. The fluctuations around the mean are represented by a zero mean, second order, stationary process.

In general, the geostatistical methods exhibit the following features: interpolates the high fidelity data, estimated values not constrained by maximum and minimum data values, and the so called *declustering*, *screening*, and *smoothing* effects. The declustering effect refers to the fact that a cluster of closely located samples will have

collectively the weight of a single sample located near the centroid of the cluster. On the other hand, the screening effect reduces the influence of a sample (original) by the addition of one or more samples at intermediate locations between the original sample and the prediction location. Furthermore, the considered geostatistical methods behave as low-pass filters away from the available data and their effect grows with the prediction error variance.

Figure 2 illustrates the Ordinary Kriging weights of sample values for estimating the high fidelity model output value at a prediction location (marked with an **X**). Note that even though samples denoted as **a**, **b** and **c**, are equally distant from the prediction location, the kriging weights for the closely located samples **b** and **c** are reduced because of the so called dec*lustering effect*; the figure also illustrates the *screening effect* in samples **d** and **e**, having the latter a negative weight. Notice how the sum of all the weights is one hence satisfying the Ordinary Kriging restriction to ensure unbiasedness.

Additionally, these methods give appraisal (error) information with the estimation, as it is shown in Figure 3. Figure 3(a) shows the estimation and prediction error standard deviation obtained at a prediction location using the KRI method. Figure 3(b), on the other hand, depicts the effect of the addition of low fidelity samples when using the CLC method; in this scenario, the prediction error standard deviation is considerably reduced at the prediction location.

The CC and CLC methods differ in whether they place restrictions on the relative position of the variable fidelity data, and on the covariance functions required. In the CC method values of the low fidelity model output have to be available at the prediction sites (exhaustive). The CLC method does not have that requirement. On the other hand, the CLC method has to fully specify a covariance function for the high and low fidelity model outputs, and for the cross-covariance between the high and low fidelity models. In contrast, the CC method does not require a covariance function for the low fidelity model. When using the CC method two different strategies are used to estimate the values of the low fidelity model at prediction locations (if necessary), namely, Ordinary kriging (CC-Kri) and the k-nn (with k=1) classifier algorithm (CC-1nn).

Table 1. *Optimization problem associated with Kriging, and Cokriging methods, and corresponding closed-form solutions*

METHOD	OPTIMIZATION FORMULATION
Ordinary Kriging	Find $\boldsymbol{\alpha}$ in: $\hat{z}_0 = a^T \boldsymbol{Z}$ such that: $Var(z_0 - \hat{z}_0) = s_Z^2 + a^T Cov(\boldsymbol{Z}) a - 2a^T Cov(\boldsymbol{Z}, z_0)$ is minimized subject to the restriction: $\sum a = 1$ to ensure unbiasedness.
	Closed-form solution is: $\hat{z}_0 = w^T IC\left(I - h\, L\, L^T IC\right)Z + h\, L^T IC\, Z$ with $L =$ Vector of ones with the same length of Z $IC = Cov(Z)^{-1}$ $h = (L^T IC\, L)^{-1}$
Classic Cokriging	Find $\boldsymbol{\alpha}$ and $\boldsymbol{\beta}$ in: $\hat{z}_0 = a^T \boldsymbol{Z} + b^T \boldsymbol{V}$ such that: $Var(z_0 - \hat{z}_0) = s_Z^2 + a^T Cov(\boldsymbol{Z}) a + b^T Cov(\boldsymbol{V}) b + 2a^T Cov(\boldsymbol{Z},\boldsymbol{V}) b - 2a^T Cov(\boldsymbol{Z}, z_0) - 2b^T Cov(\boldsymbol{V}, z_0)$ is minimized subject to the restrictions: $\sum a = 1$ and $\sum b = 0$ to ensure unbiasedness.
	Closed-form solution is: $\hat{z}_0 = \begin{bmatrix} 0 \\ 0 \\ 1 \\ 0 \end{bmatrix}^T COVAMP^{-1} \begin{bmatrix} Z \\ V \\ 0 \\ 0 \end{bmatrix} + \begin{bmatrix} Cov(Z, z_0) \\ Cov(V, z_0) \\ 0 \\ 0 \end{bmatrix}^T COVAMP^{-1} \begin{bmatrix} Z \\ V \\ 0 \\ 0 \end{bmatrix}$ with $COVAMP = \begin{bmatrix} Cov(Z) & Cov(Z,V) & L_n & 0 \\ Cov(V,Z) & Cov(V) & 0 & L_m \\ L_n^T & 0 & 0 & 0 \\ 0 & L_m^T & 0 & 0 \end{bmatrix}$ L_n y L_m are vectors of ones with the same length of Z and V respectively

Table 1. (cont.) *Optimization problem associated with Kriging, and Cokriging methods, and corresponding closed-form solutions*

METHOD	OPTIMIZATION FORMULATION
Collocated Cokriging	Find $\boldsymbol{\alpha}$ and $\boldsymbol{\beta}$ in: $\hat{z}_0 = a^T \boldsymbol{Z} + b\, v_0$ such that: $Var(z_0 - \hat{z}_0) = s_Z^2 + b^2 s_V^2 + a^T Cov(\boldsymbol{Z}) a + 2a^T Cov(\boldsymbol{Z}, v_0) b - 2a^T Cov(\boldsymbol{Z}, z_0) - 2b Cov(v_0, z_0)$ is minimized subject to the restrictions: $\left(\sum a\right) + b = 1$ to ensure unbiasedness.
	Closed-form solution is: $\hat{z}_0 = \begin{bmatrix} 0 \\ 0 \\ 1 \end{bmatrix}^T COVAMP^{-1} \begin{bmatrix} Z \\ v_0 \\ 0 \end{bmatrix} + \begin{bmatrix} Cov(Z, z_0) \\ Cov(v_0, z_0) \\ 0 \end{bmatrix}^T COVAMP^{-1} \begin{bmatrix} Z \\ v_0 \\ 0 \end{bmatrix}$ with $COVAMP = \begin{bmatrix} Cov(Z) & Cov(Z, v_0) & L_n \\ Cov(v_0, Z) & s_V^2 & 1 \\ L_n^T & 1 & 0 \end{bmatrix}$ $L_n =$ Vectors of ones with the same length of Z

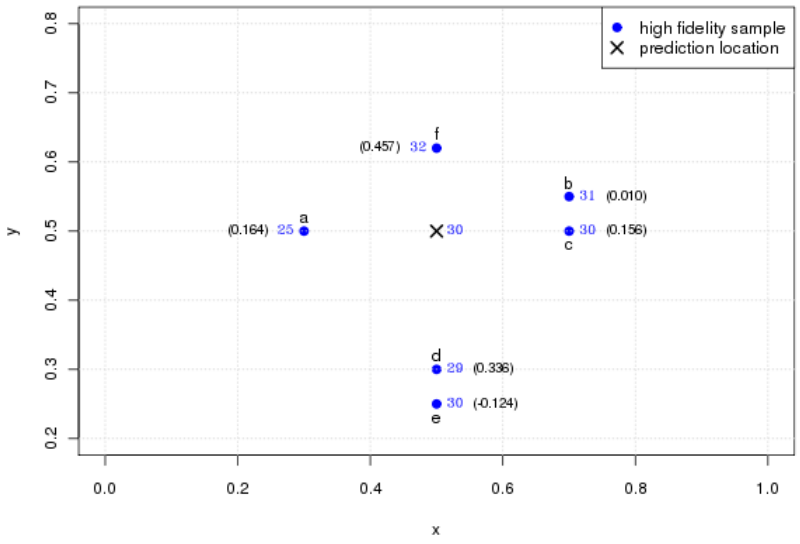

Figure 2. Ordinary Kriging weights (in parenthesis) of sample values for estimating the high fidelity model output at a prediction site (X). *The circle mark represents sample locations, and the number aside the mark denotes high fidelity model output values*

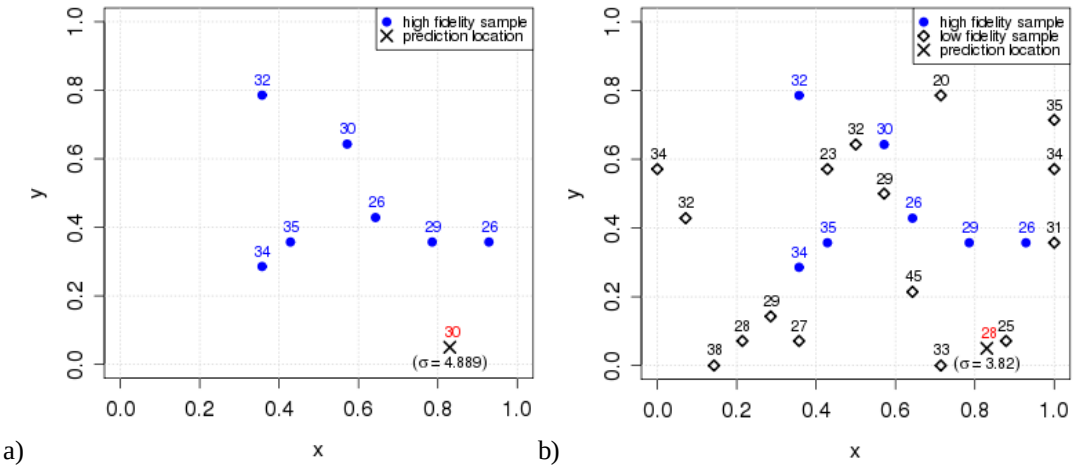

Figure 3. Estimation and prediction error standard deviation obtained at a prediction location using (a) KRI and (b) CLC methods

B. Covariance function identification

The covariance function is identified assuming the stochastic process associated with the Kriging estimates is stationary, hence, $Cov(Z_j, Z_k)$ is the same for any two points x_j, x_k, with $x_j - x_k = h$, a constant vector. More formally, in this context, the covariance between two random variables Z_j, and Z_k is defined by the following expression ($R^p \rightarrow R$):

$$Cov(Z_j, Z_k) = Cov(h) \quad \text{where} \quad h = x_j - x_k$$

When $Cov(h)$ only depends on the modulus $|h|$ and not on the direction of vector h, the stochastic process is considered isotropic and $Cov(h)$ is a scalar function ($R \rightarrow R$). In order to identify the covariance function (structure and parameters) from only a sample of model input/output pairs some additional assumptions are required; in particular, an assumption regarding the principal directions of continuity. This fact lead to the two most well-known methods for covariance function estimation: the so called DACE[16] and variogram modeling (from geostatistics) approaches (see, for example: Refs. 17-19).

The DACE approach assumes that the principal directions of continuity coincide with the cartesian axes, then, for every variable component x_j from x there is a parameter q_j that adjust the continuity (smoothness) along the j cartesian direction, and the correlation function is considered the product of a correlation function for each of the variable component in vector x, consequently, the covariance function can be specified as:

$$Cov(h) = Cov(0)\prod_{j=1}^{p} R(q_j, h_j, y)$$

where $Cov(0)$ is the process variance, the R function makes reference to the correlation structure (specified by the user) that may depend on some parameters denoted here as y. The parameters q and those in y can be specified using, for example, maximum likelihood estimates.

In contrast to the DACE approach, the variogram modeling approach looks to explore the principal directions of continuity before identifying covariance parameters. For this purpose, for vector h, a so called variogram is defined as:

$$g(h) = \frac{1}{2} E(Z_j - Z_k)^2 \quad \text{where} \quad h = x_j - x_k$$

where E denotes expected value. The basic parameters that describe a variogram are the *sill* and *range*. The *sill* is the limit of the variogram values for infinity lag (h) distances. The *range* is the lag distance where the difference

between the variogram value and the *sill* becomes negligible. Figure 4 is an example of an experimental variogram (circles) with three different theoretical model structures; the sill and range are also shown.

Considering the stationarity assumption, the covariance and variogram are related by the following expression $Cov(0) = Cov(h) + g(h)$; so if you identify the variogram, the covariance function is also established. In order to identify $Cov(h)$ using this approach another postulate needs to be made regarding the covariance anisotropy: the iso-contours of $Cov(h)$, that is, $Cov(h) = c$, are similar (with an elliptical shape) regardless of the constant *c*, and, as in principal component analysis, the orthogonal principal directions and axis sizes need to be established (e.g., using so called directional variograms). Having accomplished this task, a linear transformation takes the ellipsoids into spheres and the covariance problem is now isotropic and all the samples can be used to estimate the $Cov(h)$. The covariance model structures used are parsimonious and rely at most on only two or three parameters. Once the structure is established, the parameters (a lower number than the *p* parameters q_j in the DACE approach) can be more robustly identified using weighted mean squares, maximum likelihood, etc.

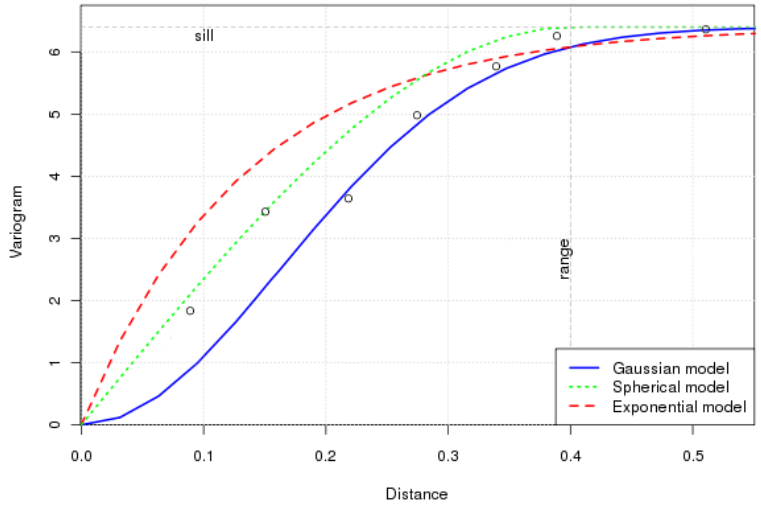

Figure 4. Example of an experimental variogram and three theoretical variograms. *The sill and range are denoted with dotted lines.*

IV. Solution methodology

The proposed approach to build a surrogate of a high fidelity model from high and low fidelity data, as specified in Section II, includes the following steps:

1) *Identify the covariance models (structure and associated parameters) required for the selected geostatistical method. In this work, for such purpose, the variogram approach is favored.* The CC method requires the identification of a covariance model associated with the high fidelity data, and, a cross covariance model for the high and low fidelity data. On the other hand, the CLC method requires not only the above-referenced covariance models but also a covariance model for the low fidelity data. Once the theoretical variogram model is identified (Table 2), the covariance model is obtained through the following expression: $Cov(h) = s^2 - \gamma(h)$, where s^2 represents the sill, $\gamma(h)$ the theoretical variogram model, and, *h* the distance between the points whose covariance is sought.

2) *If necessary, extend the low fidelity data to the prediction sites (CC method).* The cited extension can be done using kriging, or using the 1-nn classifier. In the case of kriging, a covariance function for the low fidelity model needs to be identified. Both approaches are used in the context of this work.

3) *Build a surrogate of the high fidelity model using the covariance structures/parameters identified in IV.1 as specified by the CC and CLC methods.* For a given set of prediction sites, the cokriging models require the solution of constrained optimization problems established in Table 1.

Table 2. Description of common theoretical variogram models

MODEL	$\gamma(h)/\sigma^2$	h
Nugget	0 1	$h = 0$ $h > 0$
Spherical	$\frac{3h}{2a} - \frac{1}{2}\left(\frac{h}{a}\right)^3$ 1	$0 \le h \le a$ $h > a$
Exponential	$1 - \exp\left(\frac{-h}{a}\right)$	$h \ge 0$
Gaussian	$1 - \exp\left(-\left(\frac{h}{a}\right)^2\right)$	$h \ge 0$

Given a sample of high fidelity values, the relative performance of the CC and CLC methods will be established by measuring the number of additional low fidelity values required by each of the methods to achieve different error reduction percentages with respect to the error obtained using only the initial high fidelity sample. The number of additional high fidelity values that would be required to achieve similar error reductions will also be available.

The methodology was implemented using a well-known geostatistical software package named Gstat (www.gstat.org). Available since 1997, Gstat is an open source (GPL) computer code for multivariable geostatistical modeling, prediction and simulation. As of 2003, the Gstat functionaly is also available as an S extension, either as an R package or S-Plus library. Details of Gstat can be found in Ref. 27.

V. Case studies

An analytical and an industrial case studies are used to illustrate the proposed approach and to assess the relative performance of the cokriging methods under consideration. The analytical case study corresponds to a well-known optimization test function[28] denoted as F1, and the industrial case study refers to a modeling problem in the area of enhanced oil recovery.

A. Analytical test function F1

The function of interest is represented in Equation (1). The domains of interest for the input variables x_1 and x_2 are given by the intervals (0,9), and, (0,6) respectively; the function range is 88.8.

$$F_1 = [30 + x_1 \sin(x_1)][4 + \exp(-x_2)^2] \quad (1)$$

The equation above will represent the so called high fidelity model. The low fidelity model corresponds to a filtered version of the function denoted by Equation (1) obtained using Wavelets Daubechies #4 [29]. This filtering process is expected to preserve the basic features of the original function so that the high and low fidelity models are correlated. Figure 5 illustrates both the high and low fidelity models.

The test set includes 4096 input/output pairs from a grid of 64x64.

B. Alkali-Surfactant-Polymer (ASP) modeling problem

The ASP enhanced oil recovery modeling problem addressed here is to build a surrogate model of a computationally expensive numerical simulator, that will take as input: surfactant (S) and polymer (P) concentrations, ASP slug size (expressed in the form of the injection time), and as output the cumulative oil production (NP) in bbls. The ranges of the input variables surfactant and polymer concentrations are given by $0 \le S \le 0.005$ Vol.fract. and $0 \le P \le 0.10$ wt%. The injection time is 194 days and the cumulative oil production is calculated at 800 days. As illustrated in Figure 6, the ASP flooding pilot has an inverted five-spot pattern and a total of 5 vertical wells, 4 producers and 1 injector. The high and low fidelity models are associated with two different numerical grid resolutions, namely, 18x18x3 (range: 41360 bbls), and, 9x9x3 (range: 27850 bbls) in the x, y, and z directions, respectively. The cited ranges were calculated on a 15x15 grid for the input variables (S&P). The numerical grid associated with the low fidelity model was obtained using an appropriate upscaling process.

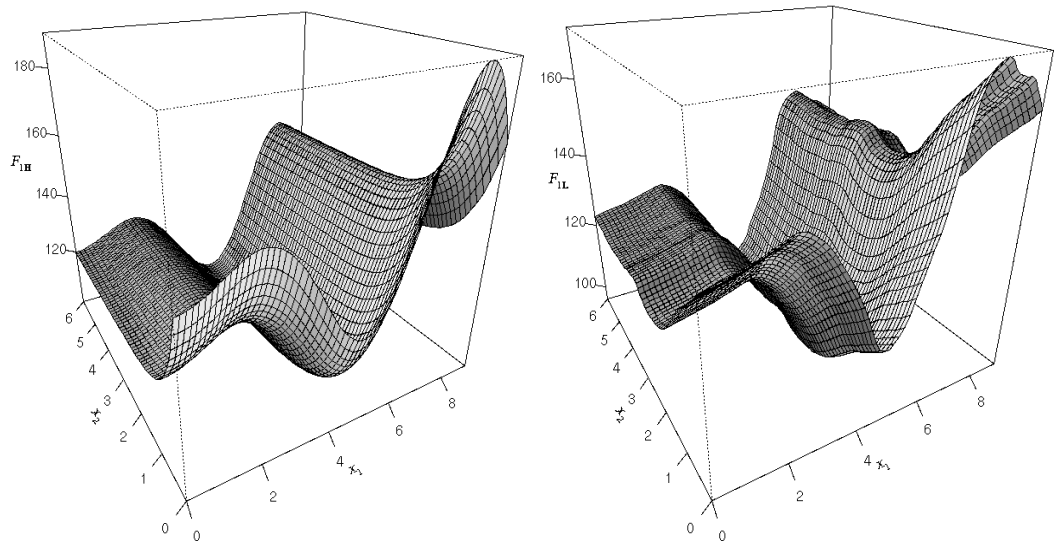

Figure 5. High (left) and low (right) fidelity models – *F1 case study*

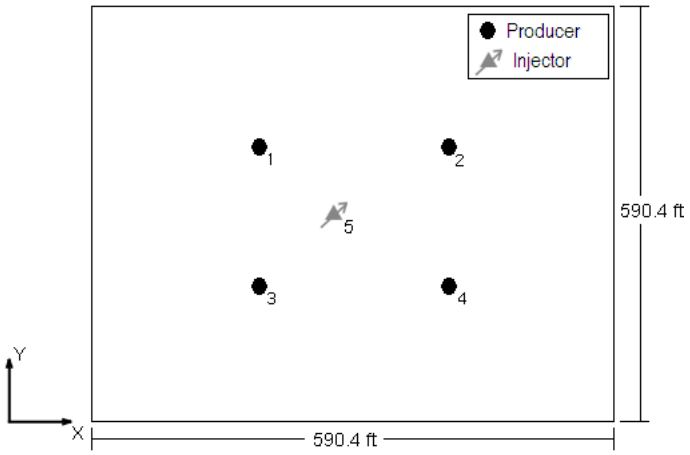

Figure 6. Inverted five-spot in the ASP flooding pilot case study

The reservoir is at a depth of 4150 ft., has an average initial pressure of 1740 psi, and the porosity is assumed to be constant throughout the reservoir and equal to 0.3. The crude oil viscosity is 40 cp, the initial brine salinity is 0.0583 meq/ml and the initial brine divalent cation concentration is 0.0025 meq/ml. A summary of the reservoir and fluid properties is presented in Table 3. The injection scheme and other reference configuration details can be found in the sample data files of the UTCHEM program[30].

The UTCHEM program is a three-dimensional, multiphase, multicomponent reservoir simulator of chemical flooding processes developed at the University of Texas at Austin[31-33]. The basic governing differential equations consist of: a mass conservation equation for each component, an overall mass conservation equation that determines the pressure (the pressure equation), an energy balance, and Darcy's Law generalized for multiphase flow. The resulting flow equations are solved using a block-centered finite-difference scheme. The solution method is implicit in pressure and explicit in concentration, similar to the well known IMPES method used in blackoil reservoir simulators. A Jacobi conjugate gradient method is used to solve the system of finite difference equations resulted from the discretization of the pressure equation.

Table 3. Reservoir and fluid properties. ASP modeling case study.

PROPERTY	VALUE	UNIT
Reservoir Depth	4150 (1265)	ft (m)
Oil viscosity	40	cp
Porosity	0.3	fraction
Average Initial Pressure	1740	psi
Well ratio	0.49 (15)	ft (m)
Skin factor	0	adim
Water Salinity	C_{Na} 0.0583 C_{Ca} 0.0025	meq/ml meq/ml

Three flowing phases and eleven components are considered in the numerical simulations. The phases are water, oil and microemulsion, while the components are water, oil, surfactant, polymer, chloride anions, divalent cations (Ca^{2+}, Mg^{2+}), carbonate, sodium, hydrogen ion, and oil acid. The ASP interactions are modeled using the reactions: in situ generated surfactant, precipitation and dissolution of minerals, cation exchange with clay and micelle, and chemical adsorption. Note the detailed chemical reaction modeling, and the heterogeneous and multiphase petroleum reservoir under consideration.

The test set includes 225 input/output pairs from a grid of 15x15.

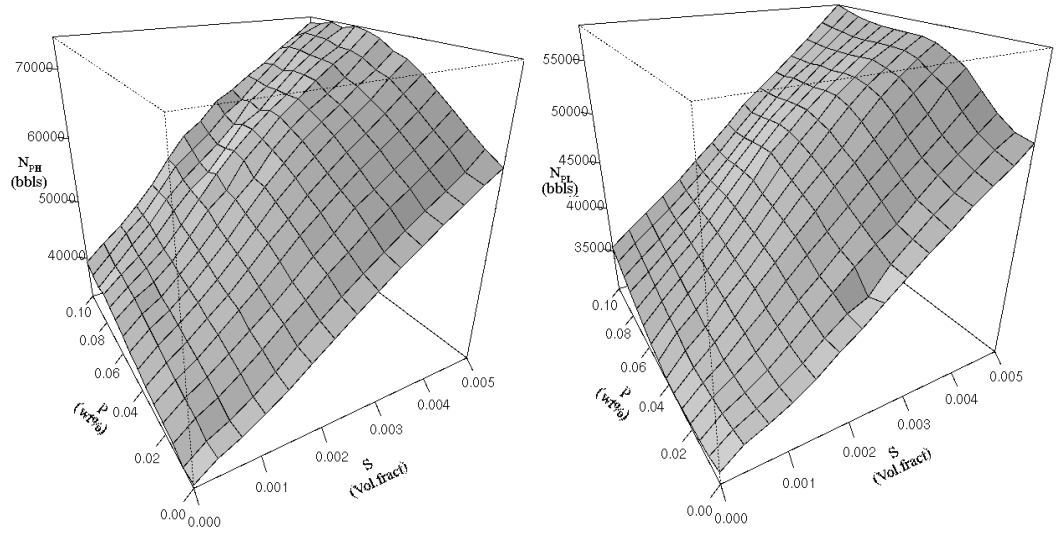

Figure 7. High (left) and low (right) fidelity models – ASP modeling case study

VI. Results and discussion

Figures 8 and 9 show the theoretical variograms associated with the high, low, and cross covariance functions adjusted to the experimental variograms in the F1 and ASP modeling case studies, respectively. The experimental variograms were constructed using an extended sample to make sure the correlation models were properly identified; specifically, for the F1 (ASP modeling) case study 90 (60) and 80 (50) high and low fidelity sample sizes were used. In all instances a single model type and range were used to assure the positive definiteness of the covariance matrices and hence a proper solution of the cokriging optimization problems. The model type that provided the best fit was the spherical model; the sill and range values for all the theoretical variograms are shown in Table 4. As expected, the sills for the low and high fidelity samples are similar, and their arithmetic mean is higher that the sill for the cross-covariance model.

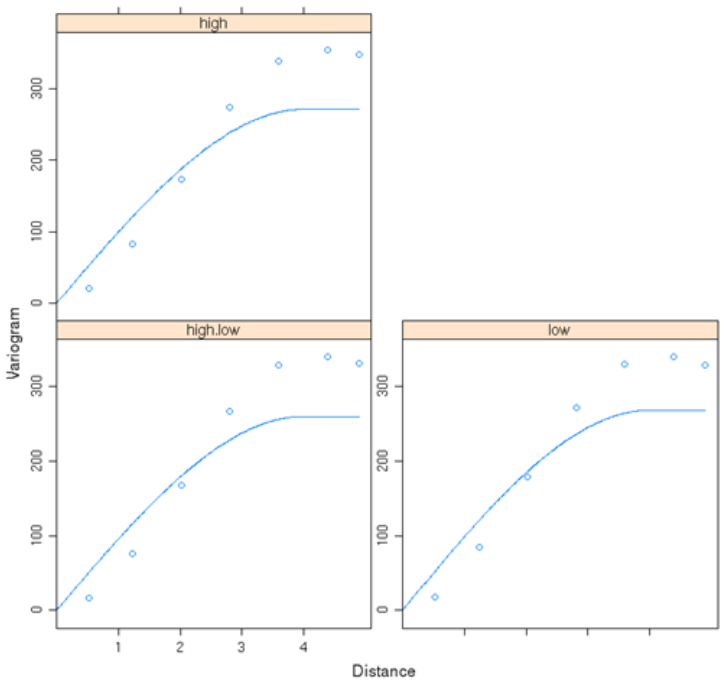

Figure 8. Theoretical variogram adjusted to the experimental variogram - F1 case study

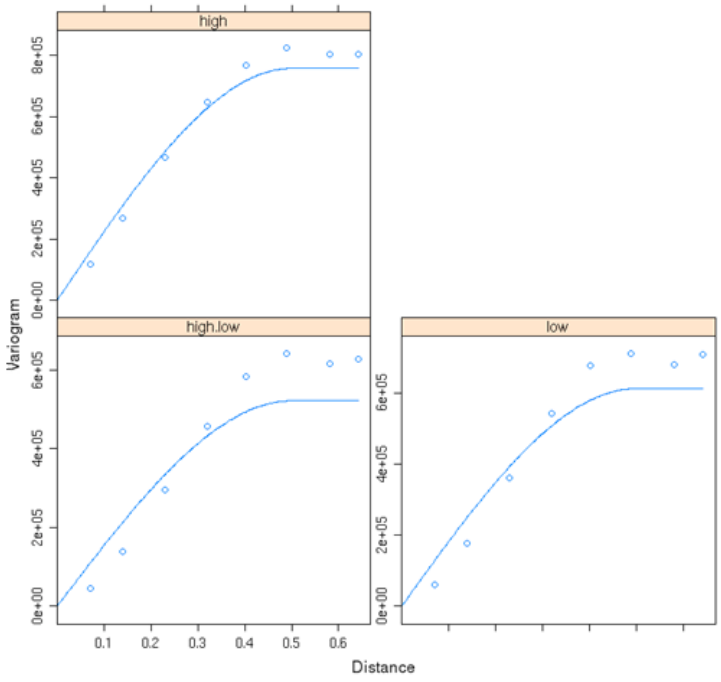

Figure 9. Theoretical variogram adjusted to the experimental variogram – ASP modeling

Table 4. Sill and range values for the theoretical variograms identified in the F1 and ASP modeling case studies

	Models	Sill	Range
F1	High	271.4	4
	Low	268.3	4
	Crossed	259.8	4
ASP	High	756977.1	0.5
	Low	612088.3	0.5
	Crossed	521801.9	0.5

Figures 10 and 11 show for the F1, and ASP modeling case studies, respectively, the relative performance of the CC and CLC methods by establishing the number of additional low fidelity values (for a given initial sample of high fidelity values) required by each of the methods to achieve a particular RMSE. The number of additional high fidelity values required to achieve similar RMSE is also shown. Additionally, Table 5 shows the number of additional high or low fidelity values necessary to reach a particular percentage reduction of the RMSE on a test data. It also shows the number of additional low fidelity values equivalent to a single high fidelity value in terms of percentage reduction of RMSE.

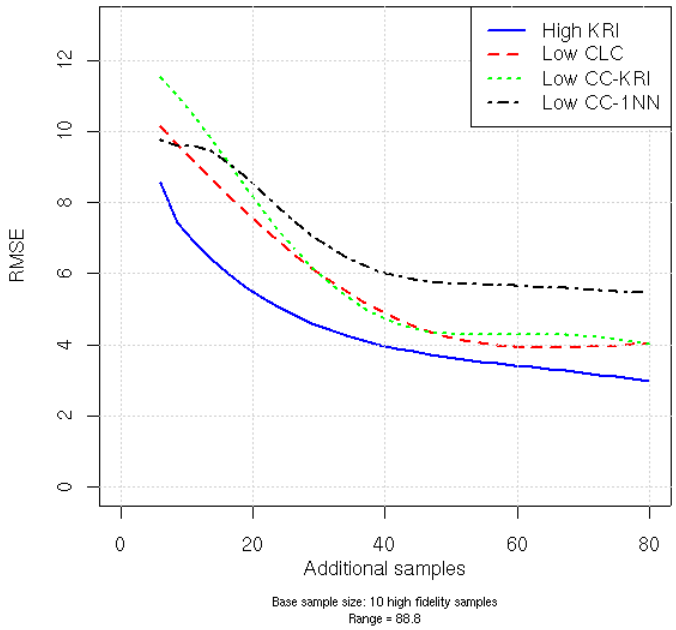

Figure 10. Number of additional low fidelity samples required for a given RMSE on a test data set for the different cokriging models. *The number of additional high fidelity samples to achieve a given RMSE is also shown (High KRI) – F1 case study.*

With reference to Figures 10 and 11, and Table 5, all the cokriging models (CLC, CC) allow improving performance by integrating low fidelity samples to an existing high fidelity one. For example, a RMSE of six (6) in the F1 case study can be achieved by the integration of approximately thirty (30) low fidelity samples using CLC or CC-Kri, or approximately fifteen (15) additional samples if only high fidelity samples are used. Similarly, in the case of the ASP modeling case study a RMSE of five hundred and fifty (550) bbls can be achieved by the integration

of approximately twenty two (22) low fidelity samples using CLC or CC-Kri, or approximately seventeen (17) additional samples if only high fidelity samples are used.

Table 5. The number of additional high or low fidelity values necessary to reach a particular percentage reduction of the RMSE on a test set. *It also shows the number of additional low fidelity values equivalent to a single high fidelity value in terms of percentage reduction of RMSE. The initial high fidelity sample size was equal to ten (10)*

Model:			CLC		CC-KRI		CC-1NN	
Case Study	% of error reduction	High fidelity samples	Low fidelity samples	Worthiness	Low fidelity samples	Worthiness	Low fidelity samples	Worthiness
F1	2	7	15	**2,14**	20	**2,86**	21	**3,00**
	4	7	16	**2,29**	20	**2,86**	22	**3,14**
	6	8	17	**2,13**	21	**2,63**	23	**2,88**
	8	8	18	**2,25**	21	**2,63**	24	**3,00**
	10	8	19	**2,38**	22	**2,75**	25	**3,13**
	12	9	20	**2,22**	23	**2,56**	26	**2,89**
	14	9	21	**2,33**	24	**2,67**	27	**3,00**
	16	10	22	**2,20**	25	**2,50**	28	**2,80**
	18	10	24	**2,40**	25	**2,50**	30	**3,00**
	20	11	25	**2,27**	26	**2,36**	31	**2,82**
	22	11	26	**2,36**	27	**2,45**	32	**2,91**
	24	12	27	**2,25**	28	**2,33**	34	**2,83**
	26	13	28	**2,15**	29	**2,23**	36	**2,77**
	28	15	30	**2,00**	30	**2,00**	38	**2,53**
	30	16	31	**1,94**	31	**1,94**	40	**2,50**
	32	17	32	**1,88**	31	**1,82**	44	**2,59**
	34	18	33	**1,83**	32	**1,78**	60	**3,33**
	36	20	35	**1,75**	34	**1,70**	74	**3,70**
	38	22	36	**1,64**	35	**1,59**	--	--
	40	24	38	**1,58**	37	**1,54**	--	--
	42	25	39	**1,56**	38	**1,52**	--	--
	44	27	41	**1,52**	40	**1,48**	--	--
	46	29	43	**1,48**	41	**1,41**	--	--
	48	31	45	**1,45**	44	**1,42**	--	--
	50	33	49	**1,48**	49	**1,48**	--	--
	52	37	52	**1,41**	76	**2,05**	--	--
	54	41	60	**1,46**	--	--	--	--
	56	45	--	--	--	--	--	--
ASP	1	7	14	**2,00**	15	**2,14**	15	**2,14**
	2	9	17	**1,89**	17	**1,89**	19	**2,11**
	3	10	18	**1,80**	18	**1,80**	21	**2,10**
	4	11	19	**1,73**	19	**1,73**	24	**2,18**
	5	12	20	**1,67**	20	**1,67**	26	**2,17**
	6	14	21	**1,50**	21	**1,50**	28	**2,00**
	7	16	23	**1,44**	22	**1,38**	31	**1,94**
	8	18	24	**1,33**	24	**1,33**	34	**1,89**
	9	20	26	**1,30**	25	**1,25**	38	**1,90**
	10	22	28	**1,27**	27	**1,23**	43	**1,95**
	11	24	30	**1,25**	29	**1,21**	50	**2,08**
	12	26	33	**1,27**	31	**1,19**	--	--
	13	28	38	**1,36**	33	**1,18**	--	--
	14	29	47	**1,62**	36	**1,24**	--	--
	15	31	--	--	45	**1,45**	--	--
	16	33	--	--	--	--	--	--

In terms of percentage reduction of RMSE (Table 5) observe that, in the F1 case study, when using CLC an eight percent (8%) reduction of the RMSE can be achieved by either eight (8) additional high fidelity values, or, eighteen (18) low fidelity ones. Hence, in this context, a high fidelity value is worth 2.25 times a low fidelity one, and, in general, the worthiness of high fidelity values decreases with increasing values of percentage reduction of the RMSE. The range of the worthiness of high fidelity values versus low fidelity ones was between 1.25 and 3.70.

Estimates of the worthiness of high fidelity values can be useful when combining a small sample of data obtained from, for example, high fidelity/computationally expensive computer simulations, and, a larger one but with low fidelity values.

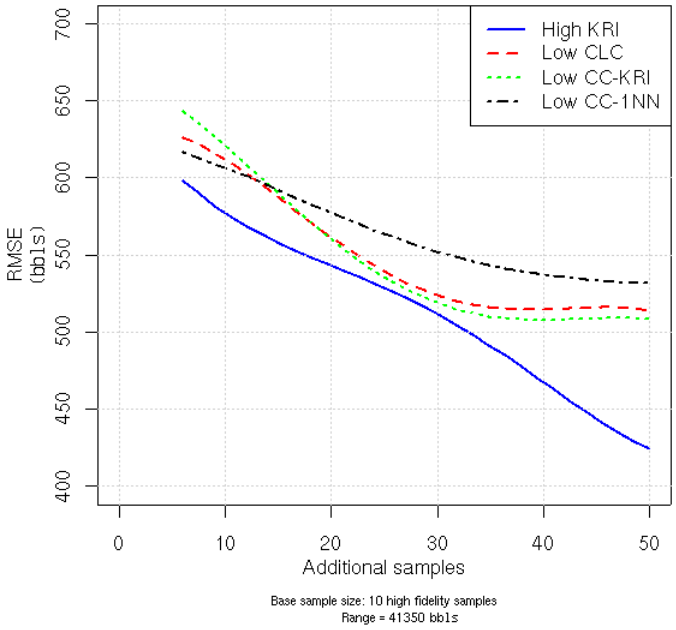

Figure 11. Number of additional low fidelity samples required for a given RMSE on a test data set for the different cokriging models. *The number of additional high fidelity samples to achieve a given RMSE is also shown (High KRI) – ASP modeling case study*

Additionally, note that for the case of low fidelity samples, after a certain sample size (problem dependent), no error reduction is observed (asymptotic behavior), which indicates that no significant modeling information is added. In general, though, this is not the case when incorporating high fidelity samples. It is also observed that the CC-Kri and CLC methods exhibited similar performance, outperforming in all instances, the CC-1nn method. For example, in the context of the ASP case study, a RMSE of five hundred and fifty (550) bbls can be achieved by the integration of approximately twenty two (22) low fidelity samples using CLC or CC-Kri, or thirty five (35) using CLC-1nn. The differences in the performance of CC-Kri vs. CC-1nn (more than 50% additional low fidelity samples required) can be explained by the latter method giving potentially inaccurate estimates when extending the low fidelity values to prediction sites.

The fact that CLC and CC-Kri exhibit similar performance is noteworthy since the former method requires the additional effort of estimating the covariance model associated with the low fidelity values; however, the performance of the latter can deteriorate if the low fidelity sample is too small to reasonably estimate the low fidelity values at prediction sites. Another consideration when selecting between the CLC and CC methods, is that if the sample size of the low fidelity variable is relatively high, the corresponding optimization problem can be significantly harder to solve in the case of the CLC method, although this latter issue can be overcome by using a restricted set of the low fidelity sample close to the prediction site.

For all case studies and cokriging approaches uncertainty estimates were consistent with amount and fidelity of the available data. For example, Figures 12 and 13 display standard deviation estimates, and uncertainty reductions throughout the input space as the result of the addition of low fidelity simples for the F1 and ASP case studies, respectively. In both cases, CLC is used and two scenarios are considered: only high fidelity simulations (10) are used (a), and both high (10) and low (10) fidelity simulations. The final picture (c) within the figures shows the uncertainty reduction as the result of the addition of low fidelity samples.

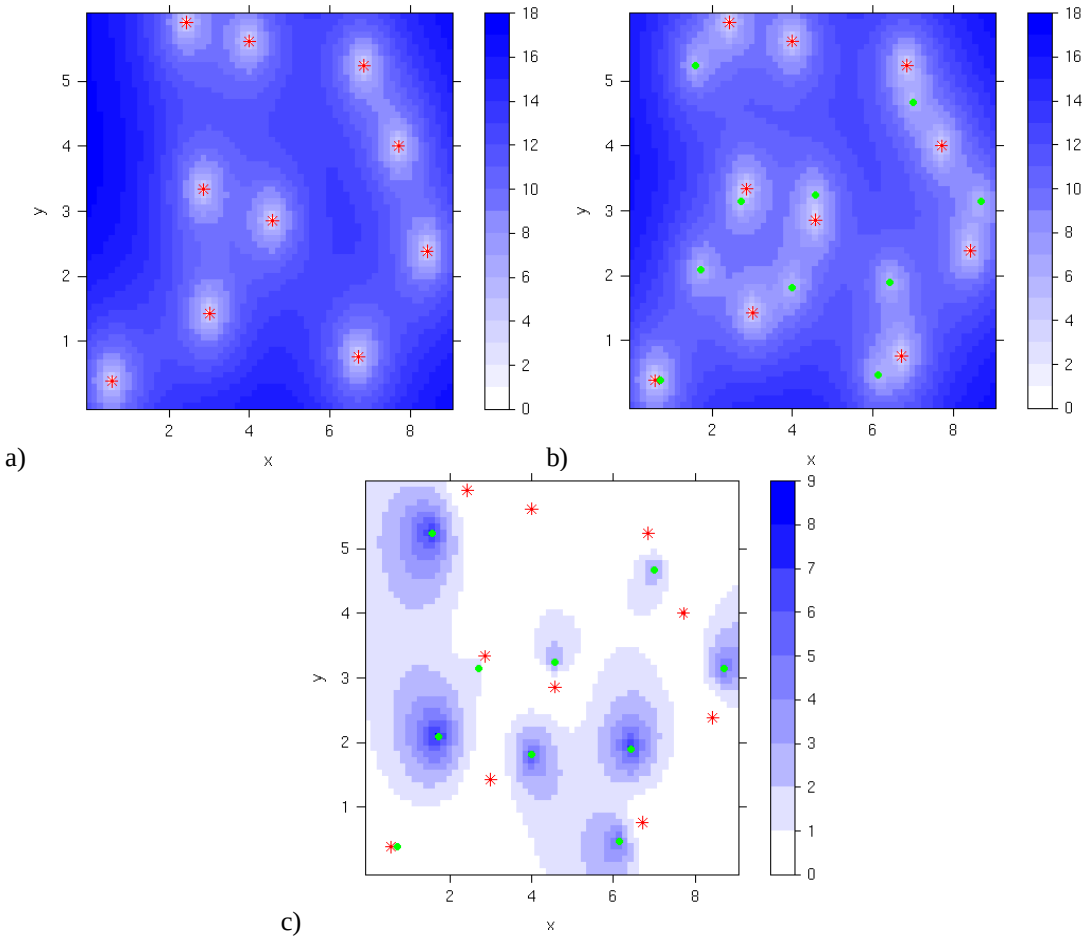

Figure 12. Standard deviation estimates (a, and b) and uncertainty reductions (c) throughout the input space as the result of the addition of low fidelity simples. *The red stars represent the location of high fidelity samples, while the green circles depict the location of low fidelity samples (F1 case study)*

With references to Figures 12(a) and 13(a) note that the standard deviation estimates goes from zero (white color) at the available data to the highest values of the scale in regions away from the available data. Also observe that the addition of low fidelity values (green circles) as shown in Figures 12(b) and 13(b) translates into lower uncertainty values (whitening of previously blue regions). Figures 12(c) and 13(c) depict that, as expected, the largest uncertainty reductions associated with the addition of low fidelity samples corresponds to regions where high fidelity values were not available.

VII. Conclusions

Ideally, surrogate models should allow: a) the integration of variable-fidelity samples, and, b) provide estimation and appraisal (error) information consistent with the amount and fidelity level of the available data. The branch of spatial statistics known as geostatistics offers considerable advantages when satisfying the above referenced requirements (a & b). This paper discussed the effectiveness and requirements of geostatistical methods such as Classic Cokriging and two variants of Collocated Cokriging for the integration of two level fidelity models; these methods can be shown to give unbiased and optimal estimates among linear models. Two case studies are considered: a well-known analytical function and, distinct resolution models, in the surrogate-based modeling of a field scale alkali-surfactant-polymer (ASP) enhanced oil recovery (EOR) process.

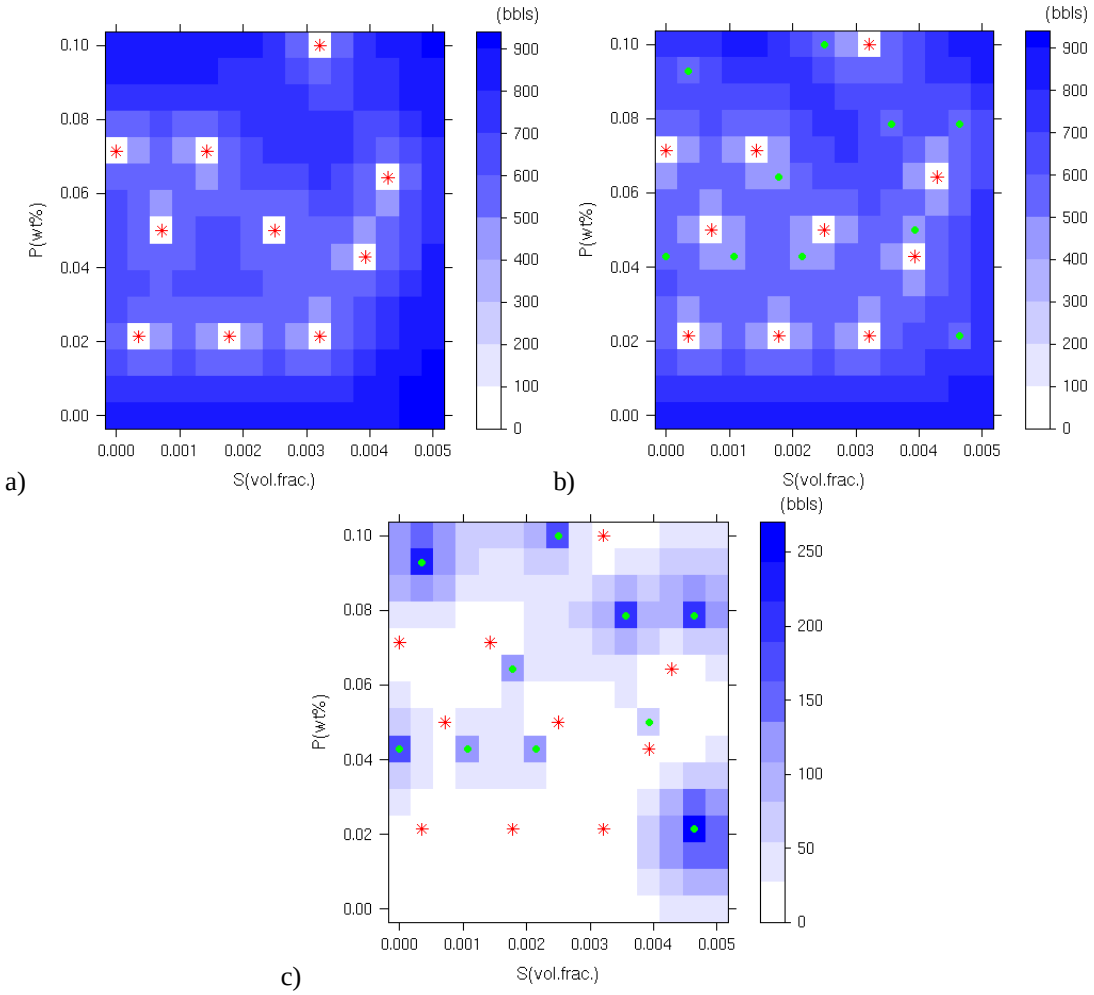

Figure 13. Standard deviation estimates (a, and b) and uncertainty reductions (c) throughout the input space as the result of the addition of low fidelity simples. *The red stars represent the location of high fidelity samples, while the green circles depict the location of low fidelity samples (ASP modeling case study)*

All Cokriging methods considered allowed improving performance by integrating low fidelity samples to an existing high fidelity one. Classic Cokriging offered the best overall performance but it has the drawback that it requires the specification of three covariance functions and the optimization formulation associated with predicting values may be hard to solve for large low fidelity sample sizes. As an alternative, the Collocated Cokriging (CC) approach does not need to specify the correlation model associated with the low fidelity values, and the optimization problem associated with the estimations are easier to solve. However, the CC approach require estimates of the low fidelity variable at prediction sites; properly extending the low fidelity value to prediction sites is sensitive to the method used and sample size. For the latter task, the kriging method showed to be much more effective than 1-nn for all samples sizes considered in this work. The Classic and Collocated Cokriging (with kriging for extending the low fidelity values to prediction sites) showed similar performance with the latter offering predictions at a significantly lower computational cost.

The cokriging approaches uncertainty estimates were consistent with amount and fidelity of the available data with the greatest uncertainty reductions associated with the addition of low fidelity samples to regions where high fidelity values were not available.

The effectiveness of the approach in the context of modeling problems in higher dimensions, the accuracy of the error variance predictions, and practical specifications of the covariance models are the subject of current research efforts.

References

[1]Giunta, A. A., Balabanov, V., Burgee, S., Grossman, B., Haftka, R. T., Mason, W. H., and Watson, L. T., "Multidisciplinary optimization of a supersonic transport using design of experiments, theory and responsive surface modeling," *Aeronautical J*, Vol. 101, 1997, pp. 347-356.

[2]Balabanov, V. O., Haftka, T., Grossma,n B., Mason, W. H. and Watson, L. T., "Multifidelity response surface model for HSCT wing bending material weight," *7th AIAA/USAF/NASA/ISSMO Symp. On Multidisciplinary Anal. and Optim.*, AIAA paper 98-4804, 1998, pp. 778-788.

[3]Li, W., and Padula, S., "Approximation methods for conceptual design of complex systems," *Eleventh Internacional Conference on Approximation Theory*, edited by Neamtu M., Schumaker K., Chui C., 2004.

[4]Queipo, N. V., Haftka, R., Shyy, W., Goel, T., Vaidyanathan, R. and Kevin, T. P., "Surrogate-based analysis and optimization," *Journal of Progress in Aerospace Sciences*, Vol. 41, 2005, pp. 1-28.

[5]Craig, K. J., Stander, N., Dooge, A. and Varadappa, S., "MDO of automotive vehicles for crashworthiness using response surface methods," *9th AIAA/ISSMO Symp. On Multidisciplinary Anal. and Optim.*, AIAA paper 2002-5607, 2002.

[6]Kurtaran, H., Eskamdarian, A., Marzougui, D. and Bedewi, N. E., "Crashworthiness design optimization using successive response surface approximations," *Computational Mechanics*, Vol. 29, 2002, pp. 409-421.

[7]Queipo, N. V., Goicochea, J., and Pintos, S., "Surrogate modeling-based optimization of SAGD processes," *Journal of Petroleum Science and Engineering*, Vol. 35, 1-2, 2002, pp. 83-93.

[8]Queipo, N. V., Verde, A., Canelon, J. and Pintos, S., "Efficient global optimization of hydraulic fractuing designs," *Journal of Petroleum Science and Engineering*, Vol. 35, 3-4, 2002, pp. 151-166.

[9]Wang, G. G., and Shan, S., "Review of metamodeling techniques in support of engineering design optimization," *Journal of Mechanical Design*, ASME, Vol. 129, Apr. 2007, pp. 370-380.

[10]Chang, K., Haftka, R., Giles, G. and Kao, P., "Sensitivity-based scaling for approximating structural response," *J. Aircraft*, Vol.30, 1993, pp. 283-287.

[11]Toropov, V., Keulen, F., Markine, V., and Alvarez, L., "Multipoint approximation based on response surface fitting: a summary of recent developments," *First ASMO UK/ISSMO*, Ilkley, UK, 1999, pp. 371-380.

[12]Vitali, R., Haftka, R., and Sankar, B., "Multifidelity design of stiffened composite panel with a crack," *Structural and Multidisciplinary Optimization*, No.23, 2002, pp. 347-356.

[13]Alexandrov, N. M., and Lewis, R. M., "An overview of first-order engineering model management for engineering optimization," *Optimization and Engineering*, Vol. 2, 2002, pp. 413-430.

[14]Bakr, M., Bandler, J., Madsen, K., and Sondergaard, J., "An introduction to the space mapping technique," *Optimization and Engineering*, Vol. 2, 2002, pp. 369-384.

[15]Bandler, J., Cheng, Q., Dakroury, S., Mohamed, A., Bak, M. and Madsen, K., "Space mapping: the state of the art," *IEEE Transactions on Microwave Theory and Techniques*, Vol. 52, 1, Jan. 2004, pp. 337-361.

[16]Sacks J., Welch W.J., Mitchell T. and Wynn H., "Design and analysis of computer experiments," *Statistical Science*, Vol. 4, No. 4, Nov. 1989, pp. 409-423.

[17]Goovaerts, P., *Geostatistics for natural resources evaluation*, Oxford, Oxford University Press, 1997.

[18] Isaaks, E., and Srivastava, R. M., *An introduction to applied geostatistics*, Oxford, Oxford Universty Press, 1989.

[19]Chiles, J. P., and Delfiner, P., *Geostatistics: Modeling spatial uncertainty*, John Wiley & Sons Inc, 1999.

[20]Kennedy, M. C., and O'Hagan, A., "Predicting the output from a complex computer code when fast approximations are available," *Biometrika*, Vol. 87, 2000, pp. 1-13.

[21]Koh-Sung, W., and Tapabrata, R., "Performance of Kriging and Cokriging based surrogate models within the unified framework for surrogate assisted optimization," *Procedings of the Congress on Evolutionary Computation (CEC'2004)*, Vol. 2, 19-23, June 2004, pp. 1577-1585.

[22]Chung, H. S., and Alonso, J., "Using gradients to construct Cokriging approximations models for high-dimensional design optimization models," *40th AIAA Aerospace Sciences Meeting and Exhibit*, AIAA paper 2002-0317, 2002.

[23]Chung, H. S., and Alonso, J., "Design of a low boom supersonic business jet using Cokriging approximation models," *9th AIAA/ISSMO Symposium on Multidisciplinary Analysis and Optimization*, AIAA paper 2002-5598, 2002.

[24]Matheron., "Principles of geostatistics," *Economic Geology*, Vol. 58, 1963, pp. 1246-1266.

[25]Sacks, J., Schiller, S., and Welch, W., "Designs for computer experiments," *Technometrics*, Vol. 31, 1989, pp. 41-47.

[26]Jones, D., Schonlau, M. and Welch, W., "Efficient global optimization of expensive black-box functions," *Journal of Global Optimization*, Vol.13, 4, 1998, pp. 455-492.

[27]GSTAT, Geostatistical modeling, prediction and simulation, Software Package, Ver. 0.9-47, Pebesma E., 2008, URL: http://www.gstat.org.

[28]Jin, R., and Chen, W., "Comparative study of metamodeling techniques under multiple modeling criteria," AIAA paper 2000-4801, 2000.

[29]Daubechies, I., "Orthonormal bases of compactly supported wavelets," *Comms. Pure Applied Math*, Vol. 41, 1988, pp. 909-996.

[30]UTCHEM three-dimensional chemical flood simulator, Software Package, Ver. 9.0., Center of petroleum and geosystems engneering, The University of Texas at Austin, 2000, URL: http://www.cpge.utexas.edu/utchem.

[31]Pope, G. A., and Nelson, R. C., "A chemical flooding compositional simulator," *Society of Petroleum Engineers*, SPE Paper 6725, 1978.

[32]Engelsen, S., Lake, L. W., Lin, E. C., Ohno, T., Pope, G. A. and Sepehrnoori, K., "Description of an improved compositional micellar/polymer simulator," *SPE Resevoir Engineering*, SPE Paper 13967, 1987, pp. 427-432.
[33]Lake, L. W., Bhuyan, D., and Pope, G. A., "Mathematical modeling of high-ph chemical flooding," *SPE Reservoir Engineering*, Vol. 5, 2, 1990, pp. 213-220.